Molecular grounds of the calculation of equilibrium and transport characteristics of inert gases and liquids in complex narrow-pore systems

Yu. K. Tovbin

State Research Center of the Russian Federation "L. Ya. Karpov Institute of Physical Chemistry", 10 ul. Vorontsovo Pole, 103064 Moscow, Russian Federation. Fax: +7 (095) 975 2450. E-mail: tovbin@cc.nifhi.ac.ru

A self-consistent approach to the calculation of equilibrium and transport characteristics of inert gases and liquids in complex narrow-pore systems based on the lattice-gas model is proposed. A supramolecular structure for fine-grained solids was constructed and the adsorbate distribution within the pore volume is described. The supramolecular structure is simulated using slit-shaped, cylindrical, spherical, and globular segments. Additionally, junctions of pore systems with different structures are included, and the heterogeneity of their walls and the presence of structural defects in the pore segments are taken into account. The distributions of molecules are described in the quasi-chemical approximation to take into account intermolecular interactions using calibration functions to correct this approximation in the near-critical area. Expressions for local and integrated flow transfer coefficients are constructed, in particular, self-diffusion, shear viscosity and heat conductivity. The contributions of the near-wall areas and the core parts of pores to the general form of phase diagrams, the effect of the pore size on the conditions of capillary condensation, and the role of surface mobility of molecules are discussed.

Key words: adsorbents, fine-grained solids, adsorption isotherm, self-diffusion coefficient, shear viscosity coefficient, heat conductivity coefficient, lattice-gas model, quasi-chemical approximation.

The transport of molecules in porous solids plays an important role in a broad range of processes, in particular, catalysis, sorption, membrane processes, *etc*.[1—7] The transport characteristics are closely related to the local densities of the adsorbate. The density of the adsorbate can vary over wide limits, and taking into account the phase transformations (capillary condensation) is a highly complicated problem both in the theory of molecular transfer and in the calculation of equilibrium characteristics of adsorption.

For most engineering processes, fine-grained solids (adsorbents, catalysts, *etc*.) with a developed specific surface and, correspondingly, with narrow pores are most important. In narrow pores, the potential of pore walls changes the conditions of capillary condensation by decreasing the critical temperature.[8—11] These conditions depend appreciably on the structure of the porous system. First of all, the characteristic size of pores is of fundamental importance. The conditions of adsorbate condensation are also affected by the heterogeneity of pore walls[12] and by the form of the pore size distribution function. In turn, the adsorbate phase distribution and the structure of the porous system influence all the dynamic characteristics of the adsorbate.

Unlike the equilibrium adsorption theory[13—17] or nonequilibrium theory for rarefied gases,[18—20] the nonequilibrium theory for dense gases and liquids has been poorly developed. At present, the flows of gaseous and liquid phases in porous systems are mainly described using homogeneous models with empirical dependences such as the Darcy law, while mass, momentum, and energy transfer in separate pores are considered using various simplified versions of the Navier—Stokes equation.[3,7,21—24] Idealized flow models in which many coefficients are taken from experiments are used most often for wide pores (or channels). For example, theoretical research at the macropore level makes use of a "mass+spring" mechanical model,[25—27] which describes the dynamics of interaction of compressible vapor (gas) shells with heavy plugs of an incompressible liquid (experimental setup of the shock wave type is used). Depending on the relationship between the free path of molecules and the characteristic pore size (pore radius for cylindrical pores and pore width for slit-shaped pores), one or another flow mechanism predominates. For long pores, the flow mechanism might change along the pore length, for example, a viscous flow at the inlet and a free-molecule flow at the outlet.[2,28]

Published in Russian in *Izvestiya Akademii Nauk. Seriya Khimicheskaya,* No. 4, pp. 827—838, April, 2003.

1066-5285/03/5204-869 $25.00

Equations and models of transport processes used for narrow pores are often[2—7,21—24] the same as those used for wide pores where the influence of pore walls on the mechanisms of transport of a dense gaseous or liquid phase can be neglected. However, in narrow pores, the surface potential becomes so significant that this approach is ill-founded. The exceptional complexity of construction of a molecular theory for the transport of molecules in narrow pores is due to highly anisotropic distribution of molecules over the pore cross-section. This has been demonstrated using all the modern methods, namely, Monte Carlo method, molecular dynamics, lattice-gas model, and the density functional theory.[13,15,29]

The molecular dynamics method allows one to study molecular flows; however, it is a very time-consuming technique, even with modern powerful computers.[30—32] A combined approach using both the molecular dynamics and Monte Carlo techniques proved to be more efficient regarding time consumption.[33] However, the applicability of this approach is still limited due to the long time required for calculations. Recently, methods for calculating the flows of dense gases and liquids in narrow pores with sizes not exceeding 10—15 nm have been developed on the basis of the lattice-gas model.[34—38] However, they are limited to an ideal geometry of slit-shaped or cylindrical pores. Therefore, it appears natural to extend the lattice-gas model to more complex porous systems. For this purpose, methods of calculation of the equilibrium distributions, phase diagrams, and transfer coefficients (self-diffusion, shear viscosity, and heat conductivity coefficients) should be made more general.

Phase diagrams for the vapor—liquid condensation of one-component systems are characterized by segregation curves, which are shaped like domes in the temperature—adsorbate density coordinates. The top of each dome corresponds to the critical temperature and density. The number of domes in the phase diagram for narrow pores depends on the adsorbate—adsorbate and adsorbate—adsorbent interaction potentials.

The Monte Carlo, molecular dynamics, density functional, and lattice-gas approaches applied to spherically symmetrical and short-chain molecules of the adsorbate gave roughly the same results for the dome properties for simple slit-shaped and cylindrical pores, which is related to the filling of the core part of the pore.[15,39—41] It was found that segregation curves for weak interaction between the adsorbate and the walls look the same way as those for the bulk phase, while in the case of strong interaction, critical densities shift toward the density of the liquid phase. The pattern of this change depends on the relationship between the interactions of the adsorbate molecules with the walls and with neighboring molecules.[39,42] However, calculations of phase diagrams for complex porous systems are few, and the diagrams available for globular systems constructed using various theoretical methods differ from one another in many respects.[43—45]

Despite the existence of a classification that comprises up to 15 variants of porous systems,[46] in the general case, one can conventionally distinguish three main types of model views on complex porous systems:

(1) a model involving the pore size distribution for infinitely long cylindrical pores (the contributions of the end effects and the connection of pores are neglected);[3]

(2) a lattice model with a regular arrangement of channels;[3,47] and

(3) a model of branching pores.[7]

Of prime importance for calculating the dynamic characteristics is to take into account the interconnection of pores of different sizes in complex systems. This component is considered in the lattice model with a regular arrangement of channels and in the model of branching pores.

In this study, the molecular adsorption theory is extended to complex porous systems with the aim of constructing equations for self-consistent calculations of the equilibrium and dynamic characteristics. The expressions for local molecular and supramolecular equilibrium distributions of the adsorbate and dynamic characteristics are constructed using the lattice-gas model.[48] The ideas of this model are used twice, namely, (1) to describe the structure of a complex porous system (supramolecular level) and (2) to take into account intermolecular interactions in the quasi-chemical approximation (molecular level). For simplicity, we will consider only a one-component fluid.

On passing from isolated pores with an ideal geometry to a complex porous system, one should consider the following factors:

(1) the finitness of the length of a particular pore segment,

(2) the presence of transient regions (junctions) between different pore segments,

(3) the pore size distribution in a macroscopic cross-section of a porous solid,

(4) connection between pores of various types located in neighboring macroscopic cross-sections,

(5) the change in the pattern of the local distribution of molecules over the cross-sections of junctions and in conditions of the fluid capillary condensation (critical temperature and coverage), depending on the structure of the inner pore volume,

(6) influence of the local structure of the pore junctions on the fluid dynamic characteristics,

(7) orientation of the pore axis relative to the direction of the macroscopic flow of molecules with averaging of the local flows.

The first four factors correspond to the procedure of description of the pore space in complex porous systems,

while the other factoirs refer to the description of the calculated characteristics of the adsorbate.

Structure of porous solids

Supramolecular level. A real porous structure will be modeled by pore segments of a fine-grained solid having some characteristic size $L > \lambda$, where λ is the linear size related to the diameter for a spherically shaped adsorbate molecules. We will restrict our consideration to one supramolecular level, namely, the adsorbent or catalyst pellet.[49,50] Higher supramolecular levels include wide transport pores exceeding the molecular scale by a large factor. The scale L refers to the supramolecular level and the scale λ, to the molecular level. The supramolecular level includes regions of the porous solid with characteristic dimension H of a particular geometry (slit-shaped, cylindrical, or spherical geometry) where H is the width for slits, the diameter for spheres or cylinders, or the volume element of the structure in the case of globular systems, which is specified in terms of globule sizes. In the general case, $H \le L$. When $H = L$, the whole segment considered is occupied by a pore. When $H = 0$, no pore is present, which reflects the existence of dead-end pores adjacent to the given segment q.

The supramolecular structure will be specified by the distribution functions F_q (characterizing the fraction of type q segments) and F_{qp} (characterizing the probability that a p type segment is adjacent to a q type segment), $\sum_p F_{qp} = F_q$, $1 \le q,p \le T$, where T is the number of segment types in the porous body. Now we introduce the function H_{qp} as the conditional probability that a pore segment of type p adjoins a pore segment of type q (along some selected direction), $F_{qp} = F_q H_{qp}$ and $\sum_p H_{qp} = 1$. The function H_{qp} takes into account the connection of pore segments of different types at the supramolecular level. This allows one to estimate the probabilities of existence of sequences of particular types of pores by means of pair distribution functions, which are known analogs of the pair distribution functions used at the molecular level, in particular, the radial pair functions used in X-ray diffraction analysis. The function H_{qp} is a full analog of the functions $d_{fg}(1)$ used for the neighboring units of a heterogeneous system at the molecular level[48] to estimate the conditional probability that a type g unit is located near a type f unit.

As an example of a complex porous system, Fig. 1 shows a system consisting of spheres and cylinders of different diameters; the distance between the sphere centers is given by $L = 30\lambda$. The cylinder radii vary from 1λ to 8λ and the sphere radii range from 9λ to 15λ. A uniform pore size distribution is assumed for both types of segments. Figure 1 represents an extension of the two-dimensional pattern[47] to the three-dimensional case. These complex porous structures can model a diversity of porous systems starting from zeolite cavities approximated by spheres with relatively short cylindrical sections of different diameters to junctions (crossings) of long cylindrical sections in new mesoporous materials such as MCM-41 and MCM-49.[51,52]

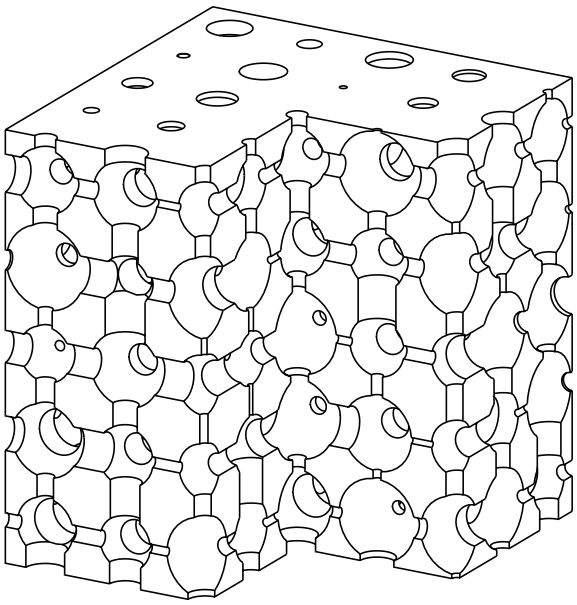

Fig. 1. Complex system of spheres and cylinders with different sizes. The distance between the sphere centers is given by $L = 30\lambda$, the sphere radii R_s vary from 9λ to 15λ, and the cylinder radii R_c are from 1λ to 8λ (the distributions of spheres and cylinders are uniform).

Molecular level. At the molecular level, the lattice-gas model[48] takes into account the intrinsic volume of the molecules and the interactions between them (the quasi-chemical and mean-field approximations are used most widely). The model is applicable over broad ranges of fluid concentrations and temperatures. For pores with a simple geometry, the model provides phase diagrams consistent with those obtained using molecular dynamics and Monte Carlo methods.[40,41] The quasi-chemical approximation ensures a qualitative agreement with precise calculations for the near-critical temperature region; therefore, calibration functions can be used to improve its accuracy around the critical points of the segregation curves.[53,54] The structure of junctions between the neighboring pore segments reflects their connection at the molecular level. By taking junctions into account, one can describe the structural defects of neighboring pore segments and coordinate additionally the atomic structure of pore walls in various fragments, in particular, to describe the heterogeneity of pore walls reflecting the atomic properties of their surfaces. To take into account the properties of junctions means to increase the number of parameters of the supramolecular structure, although formally,

consideration can be limited to the indices q and p used. The necessity of introducing additional parameters should be discussed in each particular case. In the case of spherocylindrical pores (see Fig. 1), the adsorption properties of surface sections in the vicinity of a junction were calculated within the framework of the atom-atom approximation[55,56] (for more detail, see Ref. 57).

In the lattice-gas model, the whole volume available for molecules is split into elementary units with the volume $v_0 = \lambda^3$ (λ is the lattice constant) corresponding to the size of a molecule. This eliminates the possibility of double occupation of a unit with different molecules. In complex systems, the pore volume of each fragment of the supramolecular structure q is divided into the maximum number of molecules N_q that can reside there at complete coverage. In the general case, for each unit f ($1 \le f \le N_q$) of segment q, there can exist a probability of filling $\theta_{q,f}$. The unit q,f is characterized by a local Henry constant $a_{q,f} = a_{q,f}{}^0\exp(\beta Q_{q,f})$, where $\beta = (kT)^{-1}$, $Q_{q,f}$ is the energy of binding of a molecule to the pore walls, which comprises contributions of potential of the walls placed at different distances from the unit center. However, isolation of sections with an ideal structure with identical $a_{q,f}$ values and junction regions where $a_{q,f}$ values vary from one pore cross-section to another considerably reduces the set of values of the types of units $t(q)$ within segment q.

Figure 2, *a* presents the splitting of pores into a number of layers within a globular system where four globules have been removed from the central part of the fragment. One can see irregular contour lines of the layer splittings, which are obtained using the lattice-gas model. It was assumed in the construction that the surface potential influences two first near-surface monolayers.[58] Areas corresponding to contour lines of an ideal regular structure of globules packed into a three-dimensional cubic lattice can also be seen in the cross-sections. Each layer is divided into elementary units with the size v_0, which are combined to form identical groups. Their weights, designated by F_q, for different ratios of the globule diameter R_g to the molecule size λ are presented in Fig. 2, *b*. The calculations were carried out for a broad range of R_g/λ values corresponding to the most commonly used silica gels.[55] Curves *1—4* correspond to a regular structure, curves *5—8*, to a structure with partly removed globules, and curves *9—12*, to a structure with the maximum number of removed globules.

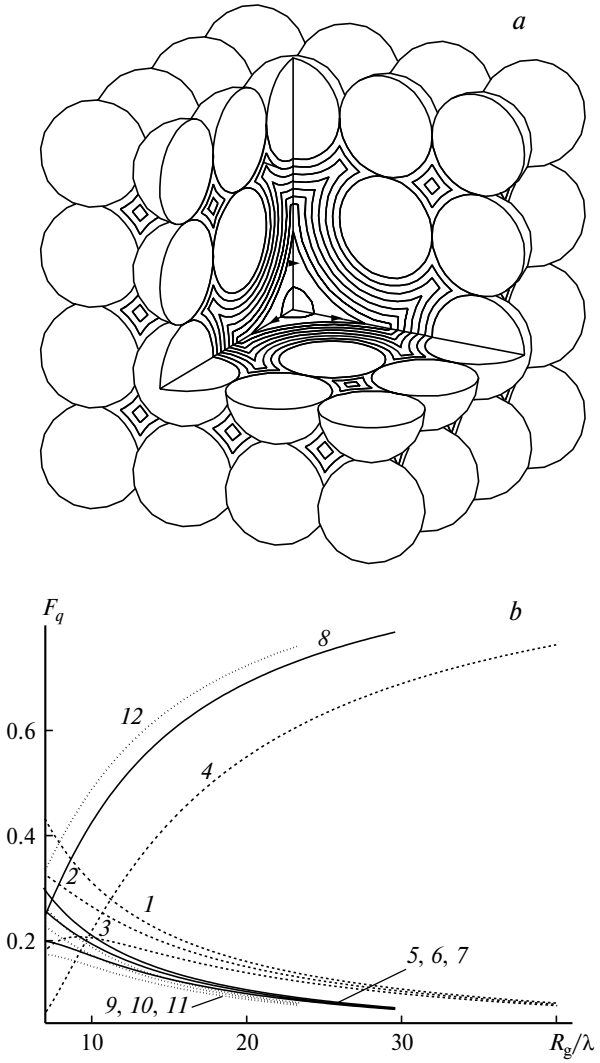

Fig. 2. (*a*) Layer cross-sections for the porous part of the globular structure. (*b*) Distribution functions F_q, for fractions of remote globules φ = 0 (*1—4*), 0.11 (*5—8*), 0.26 (*9—12*), q = 1 (curves *1*, *5*, *9*), 2 (*2*, *6*, *10*), 3 (*3*, *7*, *11*), 4 (*4*, *8*, *12*).

Equilibrium characteristics

Local isotherms. In view of the fact that each unit is specified by two indices q,f, the expressions obtained previously[48] can be used to calculate the adsorption isotherm $\theta(P)$ and the local filling of the units of different groups $\theta_{q,f}$. These expressions take into account the energetic heterogeneity of the lattice units and the interactions between the molecules at distance R of the coordination spheres:

$$\theta(P) = \sum_q F_q \sum_{f=1}^{t(q)} F_{q,f}\theta_{q,f}(P),\ a_{q,f}P = [\theta_{q,f}/(1-\theta_{q,f})]^{1+\gamma}\Lambda_{q,f},$$

$$\sum_{f=1}^{t(q)} F_{q,f} = F_q,\ \sum_{q=1}^{T} F_q = 1, \qquad (1)$$

$$\Lambda_{q,f} = \prod_r \prod_{p,g\in z_{q,f}(r)} [1 + \chi_{qp,fg}(r)t^{AA}_{qp,fg}(r)],$$

$$x_{qp,fg}(r) = \exp[-\beta\varepsilon^{AA}_{qp,fg}(r)] - 1,$$

$$t_{qp,fg}{}^{AA}(r) = 2\theta_{p,g}/[\delta_{qp,fg}(r) + b_{qp,fg}(r)],$$

$$\delta_{qp,fg}(r) = 1 + x_{qp,fg}(r)(1 - \theta_{q,f} - \theta_{p,g}),$$

$$b_{qp,fg}(r) = (\delta_{qp,fg}(r)^2 + 4x_{qp,fg}(r)\theta_{q,f}\theta_{p,g})^{1/2},$$

where $F_{q,f}$ is the fraction of units of type f for a type q pore, P is the adsorptive pressure, the function $\Lambda_{q,f}$ takes into account the imperfection of the adsorption system in the quasi-chemical approximation, and γ is the calibration function (for details, see Ref. 54). It is accepted in formula (1) that the lateral interaction parameter $\varepsilon^{AA}_{qp,fg}(r)$ of the neighboring molecules at the distance r of the coordination sphere can be a function of temperature and the local composition around units q, f and p, g. The indices p, g run over all neighbors $z_{q,f}(r)$ of unit q, f at a distance $r \le R$ inside the pore; R is the radius of the interaction potential, $R < L$.

Formula (1) describes the detailed unit distribution of all neighbors $z_{q,f}(r)$ of each unit q, f. This detailed description can be made more rough by writing the function $\Lambda_{q,f}$ in the averaged form by means of the function $F_{qp,fg}(r)$, which characterizes the probability that two units q, f and p, g are located at distance r. If all the distributions of units of different types can be approximated by the pair distribution function $H_{qp,fg}(r) = F_{qp,fg}(r)/F_{q,f}$, where $\sum_{g=1}^{t(p)} H_{qp,fg}(r) = H_{qp}$, then

$$\Lambda_{q,f} = \prod_r \left[1 + \sum_{p,g} H_{qp,fg}(r) x_{qp,fg}(r) t^{AA}_{qp,fg}(r)\right]^{z_{q,p}(r)},$$

where the subscript g refers to a segment of a type p pore. In the case of a layer distribution of the units, we obtain the following relation:

$$\Lambda_{q,f} = \prod_r \prod_{p,g} \left[1 + x_{qp,fg}(r) t^{AA}_{qp,fg}(r)\right]^{d_{qp,fg}(r)},$$

where $d_{qp,fg}(r) = z_{q,f}(r) H_{qp,fg}(r)$.

Additionally, one should take into account the normalization relations

$$\theta^{AA}_{qp,fg}(r) + \theta^{Av}_{qp,fg}(r) = \theta_{q,f} \equiv \theta_{q,f}{}^{A},$$

$$\theta^{vA}_{qp,fg}(r) + \theta^{vv}_{qp,fg}(r) = \theta_{q,f}{}^{v} = 1 - \theta_{q,f}$$

(the subscript v means a vacancy, *i.e.*, a free unit) and the fact that $\theta_{q,f}{}^{A} + \theta_{q,f}{}^{v} = 1$. The equilibrium distribution of particles over different-type units θ_k was found by solving the set of equations (1), the θ value being specified by the Newton iteration method. This set of equations can be solved with an accuracy of at least 0.1%. The densities of the coexisting gas and liquid phases of the adsorbate were determined using the Maxwell structure.[48,59]

Phase diagrams. A typical feature of the liquid—vapor segregation curves for narrow-pore systems is the presence of one or several domes corresponding to filling of near-surface layers.[42,53] Figure 3 shows the phase diagrams of the argon—silica gel system constructed assuming the same probability of filling of the central parts of different pores ($\theta_{q,t} = \theta_{p,t}$) in globular systems. Curve *1* corresponds to the initial regular structure of silica gel globules, and curve *2* refers to the same structure from which the maximum possible number of globules have been removed. An increase in the pore volume (curve *2*) increases the width of the central dome corresponding to the volume filling of the pore and decreases the width of domes corresponding to the layer-by-layer condensation of molecules in the first and second monolayers. This alteration of domes can be seen in Fig. 2, *b*. An increase in the fraction of remote globules (when R_g/λ = const) entails an increase in the fraction of the central parts of all pores and a decrease in the fraction of near-surface units. Thus, the types of phase diagrams with several near-surface domes found previously for simple pore geometries are valid on passing to complex porous systems. Performing more precise calculations in the near-critical region using a gage function does not change the number or the width of the domes but only decreases the height.[53]

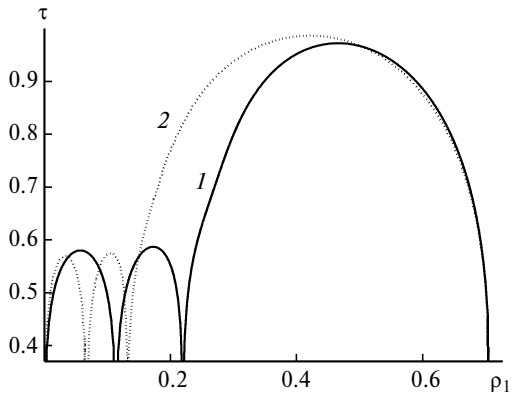

Fig. 3. Phase diagram for the argon—silica gel system ($Q_1/\varepsilon = 4$) for $R_g/\lambda = 20$; $\tau = T_c(\text{pore})/T_c(\text{bulk})$ is the reduced temperature, $\rho_1 = \theta/1.41$ is the adsorbate density expressed in the volume units of the solid spheres of the molecules. Curve *1* corresponds to a regular structure ($\varphi = 0$) and curve *2*, to the maximum removal of globules without the loss of mechanical stability of the structure ($\varphi = 0.26$) at $R_g/\lambda = 20$.

It was assumed in the calculation that the probabilities of filling of the central units and the surface units on the globule surfaces are the same. This condition depends mainly on the curvature of the globule, which determines the energy of binding of a molecule to this surface. Since R_g/λ = const, the second condition can be considered justified. However, it is well-known that the volume filling of pores of different sizes takes place at different pressures, *i.e.*, $\theta_{q,t} \neq \theta_{p,t}$. This is a basis for interpretation of the adsorption—desorption hysteresis phenomenon observed for narrow pores.[1—7,60] Therefore, it is necessary to depart from the condition of identical filling of the central units in pores of different widths.

Figure 4 shows the results of calculation of the phase diagrams for two types of segments of cylindrical pores

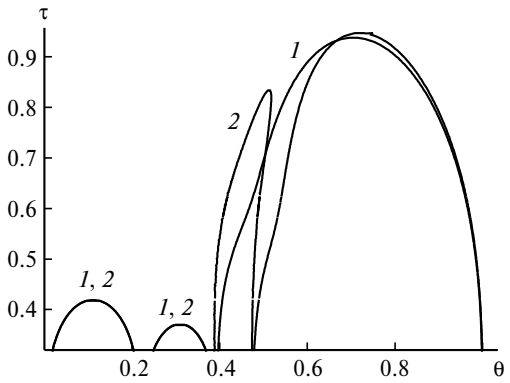

Fig. 4. Phase diagrams for a porous system containing equal proportions of two types of cylindrical pores ($F_1 = F_2$) with diameters of 10 and 20 monolayers; the calculation was done assuming that $\theta_{10,t} = \theta_{20,t}$ (*1*) and $\theta_{10,t} \neq \theta_{20,t}$ (*2*).

with the same length but different diameters in which the probability of filling of the central units was not assumed to be the same. It can be seen that the dome corresponding to the filling of the bulk parts of the porous system is split into separate domes that reflect the contributions of the fluid condensation in pores differing in size. Whereas the vapor—liquid segregation curve for simple pore geometries is split into several domes under the action of the surface potential, in complex porous systems, this curve should be additionally split into a greater number of domes due to the difference in the characteristic sizes of the pores included in the entire porous system. The number of domes observed for pores with a simple geometry is equal to the minimum possible number of domes in the phase diagram of a complex porous system. It should be emphasized that the substantial difference in the wall curvature inside the cylindrical pores, which changes the binding energy of a molecule with the walls $Q_{q,1}$, may also result in an additional splitting of near-surface domes.

This fact is important for interpretation of the adsorption—desorption hysteresis and for analysis of the transport characteristics of the adsorbate in the case where a multiphase state exists. The presence of local phases whose distribution depends on the sequence of interconnection of different-type pores with different sizes and adsorption potentials appreciably affects the observed flow characteristics.

Dynamic characteristics

Distribution functions. Now we consider the procedure of averaging of local characteristics over a sample cross-section. The expressions for transfer coefficients (self-diffusion, shear viscosity, and heat conductivity coefficients) in isolated pores obtained previously[34—36] are formally retained as the same notation. On passing from pores with a simple geometry to complex systems, one should take into account the fact that the designation of a unit has two indices characterizing the type of segment of the porous system and the number of unit in this section, as in expressions for the equilibrium distribution (1).

All the distribution functions for different pore segments introduced above refer to the whole pellet. When analyzing the transport of molecules, a flow direction from one pellet edge to another is always specified. The coordinate along the flow will be denoted by x. The pellet edges are designated by X_1 and X_2, respectively. Then the function $F_q(x)$ characterizes the fraction of type q segments in a cross-section with coordinate x along the molecular flow direction

$$\int_1^2 F_q(x)\,\mathrm{d}x = F_q,$$

where $\mathrm{d}x = \Delta x \approx L$ (the integration domain $X_1 \le x \le X_2$ is denoted by subscripts 1 and 2). The lattice parameter of the supramolecular structure serves as the minimum step at the supramolecular level. Correspondingly, instead of the pair correlation functions F_{qp} averaged throughout the sample, one must use the functions $F_{qp}(x,y)$ averaged for the neighboring cross-sections x and $y = x \pm 1$, where $|x - y| \approx L$. Let us determine the conditional probability $H_{qp}(x,y) = F_{qp}(x,y)/F_q(x)$. The following normalization relations hold for the introduced functions:

$$\int_1^2 F_{qp}(x,y)\,\mathrm{d}x\mathrm{d}y = F_{qp}, \sum_{p=1}^{T} H_{qp}(x,y) = 1.$$

When solving dynamic problems, one should also define the distribution function at the molecular level:[61,62] $F_{q,f}(x)$ characterizes the fraction of units of type f in the segment q in cross-section x, while $F_{qp,fg}(r|xy)$ defines the fraction of neighboring pairs of units q,f in cross-section x and units p, g in cross-section y at distance r with obvious normalization links

$$\int_1^2 F_{q,f}(x)\,\mathrm{d}x = F_{q,f}, \int_1^2 F_{qp,fg}(r|xy)\mathrm{d}x\mathrm{d}y = F_{qp,fg}(r).$$

In particular, the function $H_{qp,fg}(r|xy) = F_{qp,fg}(r|xy)/F_{q,f}(x)$ characterizes the conditional probability of occurrence of unit p, g in the cross-section y at distance r from the chosen unit q,f in the cross-section x. The following relations are fulfilled:

$$\int_1^2 H_{qp,fg}(r|xy)\mathrm{d}x\mathrm{d}y = H_{qp,fg}(r), \sum_{g=1}^{t(p)} H_{qp,fg}(r|xy) = H_{qp}(xy).$$

Local dynamic characteristics. The most important characteristics needed to describe the flow of molecules of one sort are self-diffusion, shear viscosity, and heat conductivity coefficients. Due to the combined influence of the adsorption potential of pore walls and intermolecu-

lar interactions, the equilibrium distributions of molecules are highly inhomogeneous across pore cross-sections. The above-mentioned coefficients are calculated with the assumption that the equilibrium distributions are slightly perturbed; therefore, they are found by solving Eqs. (1).

The equations for self-diffusion coefficients in inhomogeneous media have been derived previously.[48,61] The local self-diffusion coefficient characterizes the redistribution of molecules among neighboring units. It is calculated from the following expression:

$$D_{qp,fg}^*(\rho) = \rho^2 z^*_{qp,fg}(\rho) U_{qp,fg}(\rho)/\theta_{q,f}, \qquad (2)$$

($z^*_{qp,fg}(\rho)$ is the number of possible jumps from unit q,f to unit p,g separated by distance ρ). Here $U_{qp,fg}(\rho) = K_{qp,fg}(\rho)V_{qp,fg}(\rho)$ is the flow (the rate of molecular jumps per unit time) from unit f to unit g separated by distance ρ, which describes the rate of migration of molecules along this direction; $K_{qp,fg}(\rho)$ is the rate constant for the jumps; $V_{qp,fg}(\rho)$ is the concentration constituent of the jumping rate. According to the conventional views of the absolute reaction rate theory, this constituent depends on the relationship between the interaction energies of molecules in the ground ($\varepsilon_{AA}(r)$) and transition ($\varepsilon^*_{AA}(r)$) states. The expressions $U_{qp,fg}(\rho)$ derived from the absolute reaction rate theory for condensed phases have been described in detail in a number of publications.[34—36,48,63] When calculating the heat conductivity and heat viscosity coefficients, one should also take into account the expressions for the local self-diffusion coefficient (2).

The local heat conductivity coefficient for the transfer of the molecule energy by distance ρ along two channels (migration and collision ones) can be written in the form[64]

$$\kappa_{qp,fg}(\rho) = \theta_{q,f} C_v(q,f)[D_{qp,fg}^*(\rho) + t_{qp,fg}^{AA}(1)\lambda^2 \nu_{qp,fg}/3], \quad (3)$$

where the self-diffusion coefficient $D_{qp,fg}^*(\rho)$ is given by relation (2) and $C_v(q,f)$ is the specific heat capacity;

$$C_v(q,f) = \left(3 + \sum_{g \in z_{q,f} - \Delta_{1,f}} t_{qp,fg}^{AA}/2 + \Delta_{1;q,f}\right) k/2 + \mathrm{d}U_{q,f}/\mathrm{d}T,$$

$$U_{q,f} = 0.5 \sum_{g \in z_{q,f} - \Delta_{1;q,f}} t_{qp,fg}^{AA} \varepsilon_{qp,fg} + \Delta_{1;q,f} Q_1 + \Delta_{2;q,f} Q_2,$$

where $U_{q,f}$ is the potential energy of the molecule located in unit q,f; Δ_{ij} is the Cronecker symbol ($\Delta_{ii} = 1$ and $\Delta_{ij} = 0$ for $i \neq j$); $\nu_{qp,fg} = [48U^*(q,f)/\mu(q,f)]^{1/2}/(2\pi r_{qp,fg}^{min})$ is the harmonic oscillation frequency of the central molecule in unit q,f.

To simplify the calculations, we used[64]

(1) a pair potential like the Lennard-Jones (6—12) potential;

(2) the averaged value for the reduced mass of the adsorbate molecule in unit q,f

$$\mu(q,f)^{-1} = m^{-1}\left(\sum_{g \in z_{q,f} - \Delta_{1;q,f}} t_{qp,fg}^{AA} + 1\right) + \Delta_{1;q,f} m_s^{-1},$$

where m is the mass of the adsorbate molecule, m_s is the mass of the atom (or atoms) of the solid (adsorbent);

(3) the averaged value $U^*_{q,f}$ of the potential energy of binding of the central molecule in unit q,f:

$$U^*_{q,f} = \left(0.5 + \sum_{g \in z_{q,f} - 1 - \Delta_{1;q,f}} t_{qp,fg}^{AA} + 1\right) \varepsilon_{qp,fg} + \Delta_{1;q,f} Q_1 + \Delta_{2;q,f} Q_2.$$

Within the framework of the generalized Euring model,[34,65] the expression for the local shear viscosity coefficient for the fluid displacement in unit g relative to unit f by distance ρ has the following form:

$$\eta_{qp,fg}(\rho) = z^*_{qp,fg}(\rho)\eta_0 \exp[\beta E_{qp,fg}(\rho)]/V_{qp,fg}(\rho), \qquad (4)$$

where $\eta_0 = (mkT/\pi)^{1/2}/(\pi\sigma^2)$ is the viscosity of the ideal rarefied gas, m is the mass of the atom, σ is the diameter of the molecule, and $E_{qp,fg}(\rho)$ is the activation energy needed for jumping of the molecule between units q,f and p,g.

Average dynamic characteristics. Averaging the dynamic characteristics across any cross-section x ($X_1 \le x \le X_2$) is performed using the distribution function for pore segments of different types $F_q(x)$ and their pairs $F_{qp}(x,y)$. This averaging is preceded by averaging over units f and their pairs fg by means of functions $F_{q,f}(x)$ and $F_{qp,fg}(r|xy)$ along the cross-section x within each pore.

As an average characteristic of motion of the labeled molecules along the pore axis, one can use the expression for the self-diffusion coefficient

$$D^*_{av} = \sum_{\rho} \sum_{q} F_q(x) \sum_{f=1}^{t(q)} F_{q,f}(x) \sum_{p,g=1}^{t(p)} H_{qp,fg}(\rho|xy)\cos(x|qp,fg) \cdot \cdot D^*_{qp,fg}(\rho)\mathrm{d}\theta_{q,f}^*/\mathrm{d}\theta^*, \qquad (5)$$

where $\cos(x|qp,fg)$ is the cosine of the angle between the flow direction x and the direction connecting the units q,f and p,g in neighboring segments qp. Relation (5) reflects the thermal motion of labeled molecules inside the pore volume provided that the pore walls are impermeable (*i.e.*, molecules are not dissolved in pore walls). Under equilibrium distribution, the relation $\mathrm{d}\theta_{q,f}^*/\mathrm{d}\theta^* = \mathrm{d}\theta_{q,f}/\mathrm{d}\theta$ is fulfilled. The local jumping constants of molecules and local Henry´s constants are related by the formula $a_{q,f}K_{qp,fg} = a_{p,g}K_{pq,gf}$.

Unlike the transfer of molecules, the average heat conductivity coefficients of the adsorbate can be introduced

either along ($\kappa_\parallel$) or across ($\kappa_\perp$) the macroscopic flow. These coefficients are described by the relations

$$\kappa_\parallel = \sum_\rho \sum_q F_q(x) \sum_{f=1}^{t(q)} F_{q,f}(x) \sum_{p,g=1}^{t(p)} H_{qp,fg}(\rho|xy)\cos(x|qp,fg) \cdot \cdot \kappa_{qp,fg}(\rho), \quad (6)$$

$$\kappa_\perp = \sum_\rho \sum_q F_q(x) \sum_{f=1}^{t(q)} F_{q,f}(x) \sum_{p,g=1}^{t(p)} H_{qp,fg}(\rho|xy)\sin(x|qp,fg) \cdot \cdot \kappa_{qp,fg}(\rho). \quad (7)$$

The average hydrodynamic flow velocity in narrow pores is conventionally calculated, by analogy with macrochannels, using the Darcy equation[1—7,66,67]

$$v = -K_1 \mathrm{grad}_x P/\eta, \quad (8)$$

where K_1 is the permeability coefficient (in m^2), $\mathrm{grad}_x P$ is the pressure gradient along the direction x. The average volume flow rate of a gas or a liquid is calculated by the Hagen—Poiseuille equation

$$Q = K_2 R^n (1 + m d_{\mathrm{slip}})/\eta, \quad K_2 = K_3 \mathrm{grad}_x P, \quad (9)$$

where R is the channel radius, K_3, n, and M are numerical constants depending on the channel shape: for a cylinder, $m = n = 4$ and $K_3 = \pi/8$; for an extended slit with the width H and the length W at the inlet, we have $R = H/2$, $m = 1$, $n = 3$, $K_3 = 2W/3$, and d_{slip} is the contribution of the wall flow.[66] In the description of the momentum transfer, a constant viscosity (η) of a liquid or a gas appears in the Darsy law equation (8) for a porous system and in the Hagen—Poiseuille equation (9) for a separate pore.

Calculations based on the lattice-gas model for isolated pores with different geometries showed[42,64,65,68,69] that all the transfer coefficients are functions of the distance from pore walls and of the molecular flow direction (*i.e.*, they are tensor values). However, in derivation of Eqs. (8) and (9), the invariability of η is of prime importance. Therefore, in order to compare the results obtained for a heterogeneous fluid flow with the conclusions derived from the Darsy and Hagen—Poiseuille equations, one must introduce a mean shear viscosity coefficient along the chosen flow direction in the grain. This can be done in two ways. Expression (4) can be formally averaged across the pore cross-section provided that the pore walls are impermeable. Then by analogy with relation (5), we have

$$\eta_{\mathrm{av}} = \sum_\rho \sum_q F_q(x) \sum_{f=1}^{t(q)} F_{q,f}(x) \sum_{p,g=1}^{t(p)} H_{qp,fg}(\rho|xy)\cos(x|qp,fg) \cdot \cdot \eta_{qp,fg}(\rho). \quad (10a)$$

It can also be taken into account that the profile of the adsorbate density varies across the pore cross-section (unlike the assumptions made in deriving the Hagen—Poiseuille equation[1—7,66,67]); in this case,

$$\eta_{\mathrm{av}} = \sum_\rho \sum_q F_q(x) \sum_{f=1}^{t(q)} F_{q,f}(x) \sum_{p,g=1}^{t(p)} H_{qp,fg}(\rho|xy)\cos(x|qp,fg) \cdot \cdot \eta_{qp,fg}(\rho)\theta_{q,f}/\theta_q, \quad (10b)$$

where the factor $\theta_{q,f}/\theta_q$ renormalizes the contribution of each layer in pore f of segment q.

Contributions of particular groups of pores. The average dynamic coefficients (5)—(7) and (10) are obtained by weighing the contributions of a particular group of pores of a fixed size located in the given cross-section. The self-diffusion coefficients (5) for particular slit-shaped and cylindrical pores of different sizes have been considered in previous publications.[65,68,69] The average heat conductivity (6), (7) and shear viscosity coefficients (10) for slit-shaped pores of different widths are presented below (parameters of the second variant of intermolecular interactions were used[64]).

The average heat conductivity coefficients characterize the transfer of molecular energy along or across the macroscopic flow direction without energy exchange between the molecules and the pore walls. With an increase in the pore coverage θ (Fig. 5), the heat conductivity sharply increases because the surface layer is filled. The filling of the second layer remains low; therefore, the $\kappa_\perp$ values are much smaller than $\kappa_\parallel$ in the region of low coverages. Further increase in θ involves successive filling of the overlying layers; both components of the heat conductivity tensor approach each other and become equal for $\theta = 1$. The contribution of the surface layer decreases

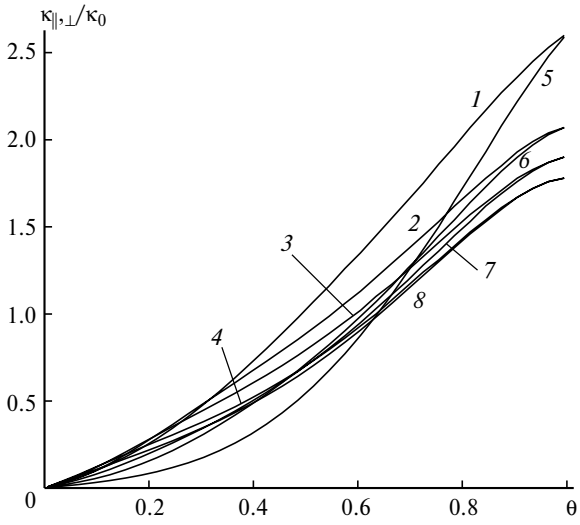

Fig. 5. Concentration dependences of the average heat conductivity coefficients of argon atoms along ($\kappa_\parallel$, curves *1—4*) and across ($\kappa_\perp$, curves *5—8*) the axis of slit-shaped carbon pores of different widths $H/\lambda = 4$ (*1*, *5*), 10 (*2*, *6*), 20 (*3*, *7*), 60 (*4*, *8*); $T = 273$ K.

with an increase in the pore width; accordingly, the curves of $\kappa_{\parallel}$ and $\kappa_{\perp}$ for higher H values move progressively downwards with the difference between them diminishing.

The relations (10) for η_{av} give an idea of the variation of the average flow viscosity coefficients in porous systems with different types of pores and characteristic sizes, although the local viscosity coefficients (4) have an obvious tensor nature.[64,65] They allow one to compare characteristics of flow viscosity used for macropores and broad capillaries with their analogs for average values in micro- and mesoporous systems. Figure 6 shows dependences (10a) for slit-shaped pores of different widths in the argon—carbon system. The concentration dependences of η_{av} for 4 to 60 monolayer wide pores are shown in Fig. 6, *a*. The average viscosity coefficient decreases with an increase in the pore width over the whole range of fillings of each pore; this reflects the decrease in the contribution of the near-surface regions where the highest viscosity is observed.

Figure 6 presents the curves for $H = 4\lambda$ and $H = 30\lambda$. The H values from 4λ to 30λ cover the whole range of "narrow pores" for spherical particles with Lennard-Jones interactions.[39,42] It can be seen that the separation between the curves depends on θ. The minimum separation is found in the θ range of ~0.2—0.3. More detailed analysis of the influence of the pore width (see Fig. 6, *b*) attests to a complex pattern of dependence of $\eta_{av}(\theta)$ on H. For low ($\theta < 0.15$) and high coverages ($\theta > 0.8$), η_{av} obeys a a linear dependence on H. Within the $0.15 < \theta < 0.8$ range, the variation of θ is accompanied by "change of the curves" with the highest average viscosity value. When $\theta \approx 0.22$, the narrowest pore $H = 4\lambda$ has the lowest viscosity. The reason for this nonlinear course of the $\eta_{av}(H)$ curves is related to the pattern of layer-by-layer filling of the pore following an increase in its width and to the fact that the dependences of η_{av}/η_0 on θ (see Fig. 6) become equal at θ = const. For an argon—carbon type system with a strong attraction to the wall, the surface layer of the adsorbate has the highest viscosity. However, its contribution to the average fluid viscosity over the pore cross-section is maximum for the overall coverage $\theta \approx 0.5$ when $H = 4\lambda$, whereas in the case of $H = 10\lambda$, the maximum value corresponds to $\theta \approx 0.2$. Therefore, the average viscosity at $\theta \approx 0.2$ is higher for $H = 10\lambda$ than for $H = 4\lambda$. However when $H > 20\lambda$, the increase in the total volume of the pore makes up for the increase in the contribution of the surface layer at relatively low θ (see Fig. 6, *a*). Qualitatively similar dependences for formula (10b) are shown in Fig. 6, *c*. However, the numerical values of the two formulas (10) are markedly different. In the case of formula (10b), the above-mentioned nonlinearity of the dependences of coefficients η_{av} on H is retained at $\theta \le 0.4$.

It has been shown[70] that local expression (4) provides a molecular-level interpretation of so-called "sliding friction coefficient β_1" in the calculation of the fluid velocity

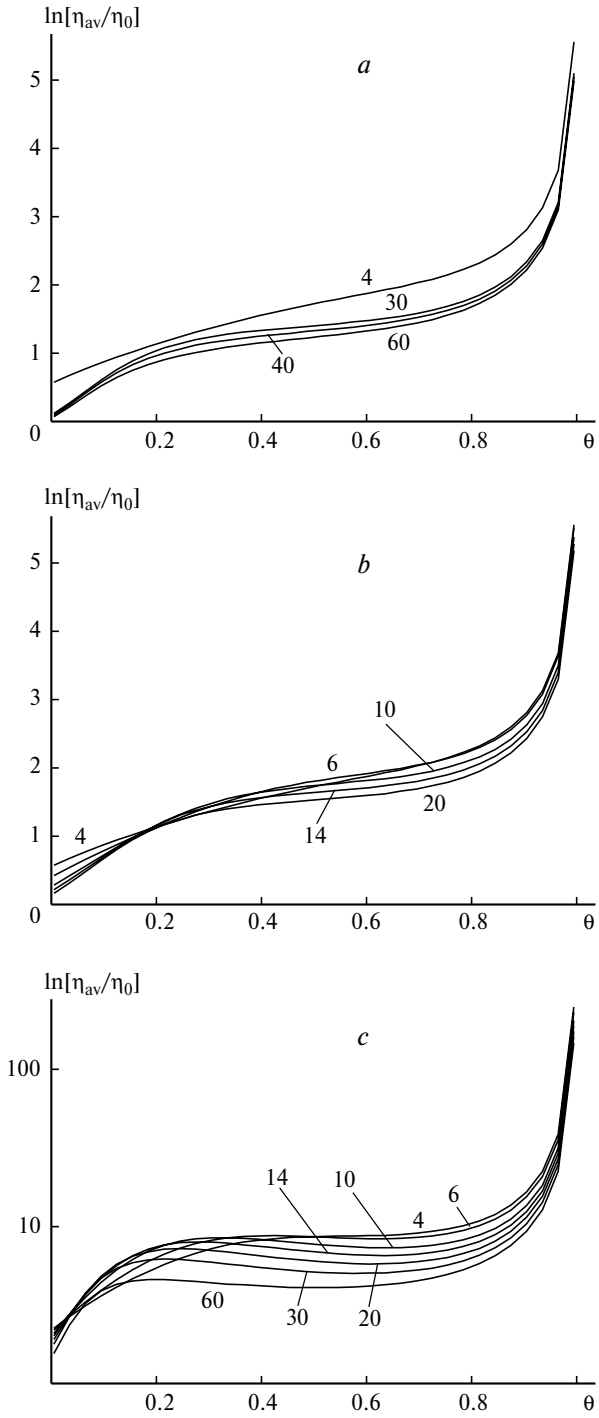

Fig. 6. Shear viscosity coefficients in separate slit-shaped pores η_{av} calculated (*a*) using formula (10a), H/λ = 4, 30, 40, 60; (*b*) formula (10a), H/λ = 4, 6, 10, 14, 20; and (*c*) formula (10b), H/λ = 4, 6, 10, 14, 20, 30, 60 (the *y*-axis scale is logarithmic).

profiles in pores (or channels) of various types.[66,67] Thus d_{slip} in formula (9) can be expressed in the dimensionless form as $d_{slip} = \eta_{tt}\lambda/(\eta_{11}R)$. In the case of strong adsorbate—adsorbent attraction or a decrease in the temperature, the η_{11}/η_{tt} ratio sharply increases according to

Eq. (4), which results in a higher coefficient β_1 and a lower flow velocity near the wall. The sliding effects have been considered previously only for rarefied gases. As opposed to the crucial role of the mirror reflection of molecules from the wall for rarefied gases, in the case of dense fluids, the sliding effect is due to the surface mobility of the molecules. It is especially important for narrow pores.

Porous systems. In a study on real adsorbents, experiments are carried out with variation of conditions (ad-

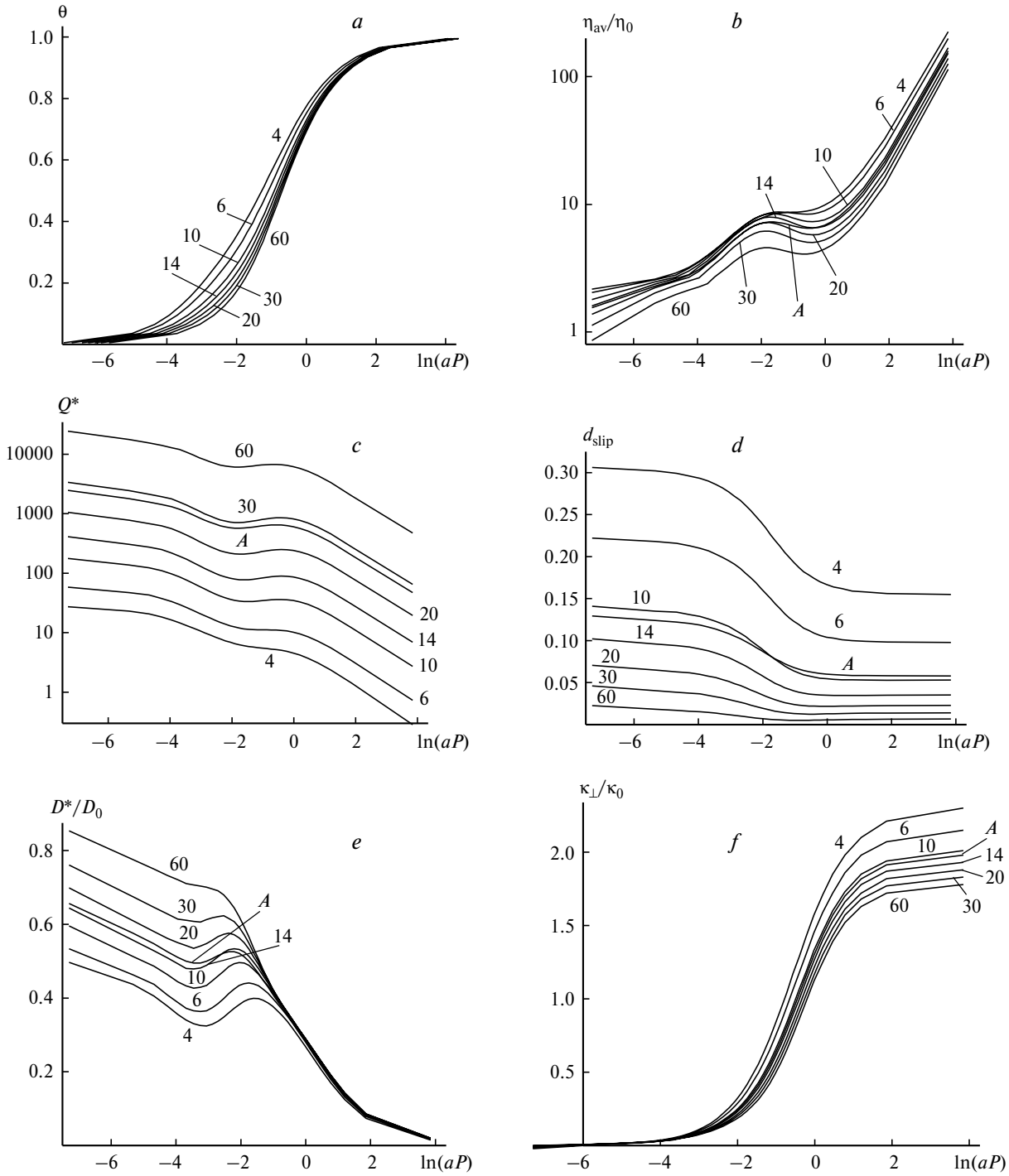

Fig. 7. Calculations of characteristics for slit-shaped pores of different widths (for explanation, see the text) and for a system with slit-shaped pores (curves *A*): adsorption isotherm (*a*); average normalized shear viscosity values calculated from formula (10b) (*b*); normalized steady-state flow rate $Q^* = Q/K_2$ (*c*); function d_{slip} (*d*); average normalized self-diffusion coefficients (*c*); normal component of heat conductivity (*f*); the *y*-axis scales in Figs. *b* and *c* are logarithmic.

sorptive temperature and pressure). Pores of different widths are filled simultaneously, the observed isotherm corresponding to the average of coverages of different pores at a specified pressure. Similarly, all the dynamic characteristics of the system are related to a specified external pressure. This means that the pressure P rather than the coverage of a given pore should generally serve as the argument of the dynamic functions for a porous system. The relationship between the external pressure and the coverages of different pores $\theta(H)$ is given by isotherms referring to pores with different widths for $\ln(aP) = \text{const}$ (Fig. 7, *a*). The concentration dependences of the main dynamic characteristics become particularly clear in Fig. 7. Figure 7 shows the concentration curves for the following parameters: adsorption isotherms, average normalized shear viscosity values calculated from formula (10b), normalized steady-state flow rate $Q^* = Q/K_2$, the function d_{slip} characterizing the contribution of the sliding effect to the overall substance flow, the average normalized self-diffusion coefficients, and the normal component of heat conductivity. Normalization was done to the volume values of the corresponding coefficients for the gas phase (as in Figs. 5 and 6). This figure shows the curves corresponding both to the narrow-pore region with fixed $H/\lambda = 4$, 6, 10, 14, 20, 30 and to $H = 60\lambda$, which is twice as great as the width of the narrow-pore region, and the mean curve A obtained by averaging with the distribution function F_q being evenly distributed over all even H/λ values ranging from 2 to 30 with additional inclusion of pores with $H/\lambda = 60$.

It can be seen from Fig. 7, *b* that the nonmonotonic pattern of dependence of the average viscosity on H (see Fig. 6) is retained in the range $H = (4—20)\lambda$. This hampers the construction of any empirical correlations between H and η (curve A is located between $H/\lambda = 14$ and 20). As the adsorbate pressure (density) increases, the steady-state flow diminishes due to an increase in the viscosity (see Fig. 7, *c*). In the $\ln(aP)$ range from -2 to 0, nonmonotonic $Q^*(\theta)$ is observed. For this dependence, curve A lies somewhat below the curve for $H = 30\lambda$, whereas in the case of the d_{slip} dependence (see Fig. 7, *d*), it runs in the vicinity of $H = 10\lambda$. The curves in Fig. 7, *d* indicate that for all pores referred to as narrow ones, the sliding effect makes a noticeable contribution to the total flow (9). The results of calculation of d_{slip} refer to relatively low activation energy for the migration of molecules in the surface layer where $E_{11} = Q_1/3$. It is evident that the contribution of d_{slip} will decrease with an increase in the pore width.

Figure 7, *e* shows how the self-diffusion coefficients in different pores change with an increase in the adsorbate pressure. The maximum at $\ln(aP) \approx -2$ corresponding to filling of the surface monolayer is present for the whole range of narrow pores but is absent for $H = 60\lambda$. The self-diffusion coefficient decreases substantially as the pressure increases from gas-phase to liquid-phase values. Conversely, the heat conductivity coefficient across the molecular flow increases monotonically with an increase in pressure. Curves A in Figs. 7, *e* and 7, *f* are located near $H = 14\lambda$ for the self-diffusion coefficient and between $H = 10\lambda$ and $H = 14\lambda$ for the heat conductivity coefficient $\kappa_\perp$.

All the averaged curves A (see Fig 7) corresponding to the porous system as a whole are located in different regions of H values. This is due to individual relations between the properties of the considered characteristics and the pore width. This specificity hampers the search for versatile relations involving averaged characteristics and calls for specific numerical analysis of each porous system under interest.

* * *

Thus, the extension of the lattice-gas model considered here allows one to pass to a self-consistent calculation of equilibrium and dynamic characteristics in narrow-pore systems. The formulated molecular approach can be used to study the effect of the adsorbate—adsorbent and adsorbate—adsorbate potentials on the observed characteristics over broad ranges of adsorptive temperatures and pressures. The allowance made for seven factors in order to pass from idealized pores with an infinite length to complex porous systems changes the results obtained previously for separate pores.[39—42,68,69] Taking into account the finitness of the three linear dimensions of each local segment of pores would have a substantial influence on the conditions of distribution of molecules in pore mouths, and the size of the transient regions between different pore segments would influence the formation of the types of segments at the supramolecular level, in particular, on the pore size distribution (function F_q) and pore interconnection (function F_{qp}). The array of interconnected pore segments forms a common pore volume, the pattern of local distributions of the adsorbate in any part of the system affects the distribution of molecules in the neighboring pore segments. As a consequence, the possibility and the critical conditions (temperatures and coverages) of the occurrence of capillary condensation depend on the properties of some fragments of the interpore space, which, in turn, depends on functions F_q and F_{qp}. The introduction of functions F_{qp} is of prime importance for the dynamic description because the interconnected sequences of the through pores segments are important for the molecular transport. The derived expressions for dynamic characteristics (5)—(7) and (10) take into account the pattern of pore junction.

In real adsorbents and catalysts with a continuous pore size distribution, the phase state of the adsorbate also depends on the pore size in a given local region of the adsorbent and on the pore sizes in the regions surround-

ing the given region. As a consequence, calculation of phase distributions of the adsorbate and their dynamic characteristics requires extending the above discrete functions F_q and F_{qp} to continuous ones (this is attained by natural replacement of sums by integrals by analogy with the transition to continuous functions for the coordinate x along the grain size). Thus, a substantial portion of the information is represented not only by the pore size distribution function but also by a function characterizing the structure of the internal pore volume of the adsorbent. The same situation should arise in the description of the pore space structure for a supramolecular level higher than the adsorbent/catalyst pellet.

This work was financially supported by the Russian Foundation for Basic Research (Project No. 00-03-32153).

References

1. B. V. Deryagin, N. V. Churaev, and V. M. Muller, *Poverkhnostnye sily* [*Surface Forces*], Nauka, Moscow, 1985, 400 pp. (in Russian).
2. D. P. Timofeev, *Kinetika adsorbtsii* [*Adsorption Kinetics*], Izd-vo Akad. Nauk SSSR, Moscow, 1962, 252 pp. (in Russian).
3. L. I. Kheifets and A. V. Neimark, *Mnogofaznye protsessy v poristykh sredakh* [*Multiphase Processes in Porous Media*], Khimiya, Moscow, 1982, 320 pp. (in Russian).
4. P. C. Carman, *Flow of Gases Through Porous Media*, Butterworths, London, 1956.
5. C. N. Satterfield, *Mass Transfer in Heterogeneous Catalysis*, MIT Press, Cambridge, Mass., 1970.
6. E. A. Mason and A. P. Malinauskas, *Gas Transport in Porous Media: The Dusty-Gas Model*, Elsevier, Amsterdam, 1983.
7. Yu. A. Chizmadzhev, V. S. Markin, V. R. Tarasevich, and Yu. G. Chirkov, *Makrokinetika protsessov v poristykh sredakh* [*Process Macrokinetics in Porous Mrdia*], Nauka, Moscow, 1971, 362 pp. (in Russian).
8. H. Nakanishi and M. E. Fisher, *J. Chem. Phys.*, 1983, **78**, 3279.
9. P. Tarasona, U. M. B. Marconi, and R. Evans, *Mol. Phys.*, 1987, **60**, 573.
10. A. de Kreizer, T. Michalski, and G. H. Findenegg, *Pure Appl. Chem.*, 1991, **63**, 1495.
11. Yu. K. Tovbin and E. V. Votyakov, *Langmuir*, 1993, **9**, 2652.
12. E. V. Votyakov and Yu. K. Tovbin, *Zh. Fiz. Khim.*, 1994, **68**, 287 [*Russ. J. Phys. Chem.*, 1994, **68**, No. 2 (Engl. Transl.)].
13. Yu. K. Tovbin, in *Metod molekulyarnoi dinamiki v fizicheskoi khimii* [*Molecular Dynamics Approach in Physical Chemistry*], Nauka, Moscow, 1996, 128 (in Russian).
14. *Dynamics of Gas Adsorption on Heterogeneous Solid Surfaces*, Eds. W. Rudzinski, W. A. Steele, and G. Zgrablich, Elsevier, Amsterdam, 1996.
15. L. D. Gelb, K. E. Gubbins, R. Radhakrishnan, and M. Sliwinska-Bartkowiak, *Rep. Prog. Phys.*, 1999, **62**, 1573.
16. T. G. Plachenov and S. D. Kolosentsev, *Porometriya* [*Porometry*], Khimiya, Leningrad, 1988, 176 pp. (in Russian).
17. L. Sarkisov, K. S. Page, and P. A. Monson, in *Fundamentals of Adsorption 6*, Elsevier, Paris, 1998, 847.
18. V. D. Borman, S. Yu. Krylov, and A. V. Prosyanov, *Zh. Eksperim. Teor. Fiz.*, 1990, **97**, 1795 [*J. Exp. Theor. Phys.*, 1990, **97** (Engl. Transl.)].
19. V. D. Borman, S. Yu. Krylov, A. V. Prosyanov, and A. M. Kharitonov, *Zh. Eksperim. Teor. Fiz.*, 1986, **90**, 76 [*J. Exp. Theor. Phys.*, 1986, **90** (Engl. Transl.)].
20. S. F. Borisov, N. F. Balakhonov, and V. A. Gubanov, *Vzaimodeistviya gazov s poverkhnost'yu tverdogo tela* [*Interactions of Gases with Solid Surfaces*], Nauka, Moscow, 1988, 200 pp. (in Russian).
21. R. E. Collins, *Flow of Fluid Through Porous Materials*, Reinhold Publ. Corp., New York, 1961.
22. A. E. Scheidegger, *The Physicas of Flow Through Porous Media*, Univer. Press, Toronto, 1957.
23. R. I. Nigmatulin, *Osnovy mekhaniki geterogennykh sred* [*Fundamentsls of the Mechanics of Heterogeneous Media*], Nauka, Moscow, 1973, 336 pp. (in Russian).
24. V. N. Nikolaevskii, *Mekhanika poristykh i treshchinovatykh sred* [*Mechanics of Porous and Fractured Media*], Nedra, Moscow, 1984, 232 pp. (in Russian).
25. B. G. Pokusaev, S. I. Lezhik, N. A. Pribaturin, E. S. Vasserman, and S. P. Akterov, *1-ya Ros. nats. konf. po teploobmenu*, **4**, *Dvukhfaznye techeniya* [*Ist Russ. National Conf. on Ion exchange,* **4**, *Two-phase Flows*], *Proc.*, Izd-vo MEI, Moscow, 1994, 189 pp. (in Russian).
26. V. E. Nakoryakov, B. G. Pokusaev, and N. A. Pribaturin, *Dokl. Akad. Nauk SSSR*, 1990, **311**, 1230 [*Dokl. Chem.*, 1990, **311** (Engl. Transl.)].
27. B. S. Lezhnin and B. S. Zhakunov, *1-ya Ros. nats. konf. po teploobmenu*, **4**, *Dvukhfaznye techeniya* [*1-st Russ. National Conf. on Ion exchange,* **4***, Two-phase Flows*], *Proc.*, Izd-vo MEI, Moscow, 1994, 126 (in Russian).
28. E. Wicke and W. Vollmer, *Chem. Eng. Soc.*, 1952, **1**, 282.
29. A. G. Grivtsov, in *Osnovnye problemy teorii fizicheskoi adsorbtsii* [*Key Problems of the Physical Adsorption Theory*], Nauka, Moscow, 1970, p. 352 (in Russian).
30. S. Sokolovski, *Phys. Rev., A*, 1991, **44**, 3732.
31. S. Sokolovski, *Mol. Phys.*, 1992, **75**, 1301.
32. B. J. Palmer, *J. Chem. Phys.*, 1998, **109**, 196.
33. J. M. D. MacElroy, *J. Chem. Phys.*, 1994, **101**, 5274.
34. Yu. K. Tovbin, *Zh. Fiz. Khim.*, 1998, **72**, 1446 [*Russ. J. Phys. Chem.*, 1998, **72**, No. 8 (Engl. Transl.)].
35. Yu. K. Tovbin, *Zh. Fiz. Khim.*, 2002, **76**, 76 [*Russ. J. Phys. Chem.*, 2002, **76**, No. 1 (Engl. Transl.)].
36. Yu. K. Tovbin, *Khim. Fizika*, 2002, **36**, 87 [*Russ. J. Chem. Phys.*, 2002, **36** (Engl. Transl.)].
37. Yu. K. Tovbin and R. Ya. Tugazakov, *Teoret. Osnovy Khim. Tekhnol.*, 2000, **34**, 117 [*Theor. Foundations Chem. Technol.*, 2000, **34** (Engl. Transl.)].
38. Yu. K. Tovbin and R. Ya. Tugazakov, *Teoret. Osnovy Khim. Tekhnol.*, 2002, **36**, 573 [*Theor. Foundations Chem. Technol.*, 2002, **36** (Engl. Transl.)].
39. Yu. K. Tovbin and E. V. Votyakov, *Izv. Akad. Nauk*, *Ser. Khim.*, 2001, 48 [*Russ. Chem. Bull., Int. Ed.*, 2001, **50**, 50].
40. E. V. Votyakov, Yu. K. Tovbin, J. M. D. MacElroy, and A. Roche, *Langmuir*, 1999, **15**, 5713.
41. A. M. Vishnyakov, E. M. Piotrovskaya, E. N. Brodskaya, E. V. Votyakov, and Yu. K. Tovbin, *Zh. Fiz. Khim.*, 2000, **74**, 501 [*Russ. J. Phys. Chem.*, 2000, **74**, No. 3 (Engl. Transl.)].

42. Yu. K. Tovbin, in *Mater. Konf., Posvyashchennoi 100-letiyu M. M. Dubinina* [*Proc. Conf. Dedicated to the 100th Anniv. Acad. M. M. Dubinin*], IFKh RAN, Moscow, 2001, p. 27 (in Russian).
43. E. Kierlik, M. L. Rosinberg, G. Tarjus, and P. A. Monson, *Fundamentals of Adsorption 6*, Elsevier, Paris, 1998, 867.
44. E. Kierlik, M. L. Rosinberg, G. Tarjus, and P. A. Monson, *J. Chem. Phys.*, 1997, **106**, 264.
45. Yu. K. Tovbin, *Zh. Fiz. Khim.*, 2002, **76**, 488 [*Russ. J. Phys. Chem.*, 2002, **76**, No. 4 (Engl. Transl.)].
46. J. H. de Boer, *Proc. 10th Symp. Colston Res. Soc.*, 1958, **10**, 68.
47. V. Mayagoitia, F. Rojas, and I. Kornhauser, *Langmuir*, 1993, **9**, 2748.
48. Yu. K. Tovbin, *Teoriya fiziko-khimicheskikh protsesov na granitse gaz—tverdoe telo*, Nauka, Moscow, 1990, 288 pp. [Yu. K. Tovbin, *Theory of Physical Chemistry Processes at a Gas—Solid Surface Processes*, CRC Press, Boca Raton, Fl, 1991].
49. E. Ruckenstein, A. S. Vaidyanathan, and G. R. Youngquist, *Chem. Eng. Sci.*, 1971, **26**, 1305.
50. V. Sh. Mamleev, P. P. Zolotarev, and P. P. Gladyshev, *Neodnorodnost' sorbentov* [*Sorbent Inhomogeneity*], Nauka, Alma-Ata, 1989, 287 pp. (in Russian).
51. N. Dufau, P. L. Llewellyn, C. Martin, J. P. Coulomb, and Y. Grillet, in *Fundamentals of Adsorption 6*, Elsevier, Paris, 1998, p. 63.
52. M. Grun, K. Schumacher, and K. Unger, in *Fundamentals of Adsorption 6*, Elsevier, Paris, 1998, p. 569.
53. Yu. K. Tovbin, A. B. Rabinovich, and E. V. Votyakov, *Izv. Akad. Nauk, Ser. Khim.*, 2002, 1531 [*Russ. Chem. Bull., Int. Ed.*, 2002, **51**, 1667].
54. Yu. K. Tovbin, *Zh. Fiz. Khim.*, 1998, **72**, 2254 [*Russ. J. Phys. Chem.*, 1998, **72**, No. 12 (Engl. Transl.)].
55. A. V. Kiselev, *Mezhmolekulyarnye vzaimodeistviya v adsorbtsii i khromatografii* [*Intermolecular Interactions in Adsorption and Chromatography*], Vysshaya shkola, Moscow, 1986, 360 pp. (in Russian).
56. W. A. Steele, *The Interactions of Gases with Solid Surfaces*, Pergamon, New York, 1974.
57. D. V. Eremich, V. N. Komarov, and Yu. K. Tovbin, *XIV Simp. "Sovremennaya khimicheskaya fizika" (Tuapse, 18—29 sentyabrya 2002)* [*XIV Symp. "Modern Chemical Physics" (Tuapse, September 18—29, 2002)*], *Abstrs.*, MGU, Moscow, 95 (in Russian).
58. Yu. K. Tovbin and D. V. Yeremich, *Colloids and Surfaces*, *A*, 2002, **296**, 363.
59. T. L. Hill, *Statistical Mechanics. Principles and Selected Applications*, McGraw-Hill, New York, 1956.
60. S. J. Gregg and K. G. W. Sing, *Adsorption, Surface Area, and Porosity*, Academic Press, London, 1982.
61. Yu. K. Tovbin, *Dokl. Akad. Nauk SSSR*, 1990, **312**, 1425 [*Dokl. Chem.*, 1990 (Engl. Transl.)].
62. Yu. K. Tovbin, *Zh. Fiz. Khim.*, 1997, **73**, 1454 [*Russ. J. Phys. Chem.*, 1997, **73**, No. 8 (Engl. Transl.)].
63. Yu. K. Tovbin, *Progress in Surface Science*, 1990, **34**, 1.
64. Yu. K. Tovbin and V. N. Komarov, *Izv. Akad. Nauk, Ser. Khim.*, 2002, 1871 [*Russ. Chem. Bull., Int. Ed.*, 2002, **51**, 2026].
65. Yu. K. Tovbin and N. F. Vasyutkin, *Izv. Akad. Nauk, Ser. Khim.*, 2001, 1496 [*Russ. Chem. Bull., Int. Ed.*, 2001, **50**, 1572].
66. R. B. Bird, W. Stewart, and E. N. Lightfoot, *Transport Phenomena*, J. Wiley and Sons, New York—London, 1965.
67. G. Lamb, *Hydrodynamics*, 1932.
68. Yu. K. Tovbin and N. F. Vasyutkin, *Zh. Fiz. Khim.*, 2002, **76**, 319 [*Russ. J. Phys. Chem.*, 2002, **76**, No. 2 (Engl. Transl.)].
69. Yu. K. Tovbin, E. E. Gvozdeva, and D. V. Eremich, *Zh. Fiz. Khim.*, 2003, **77**, No. 5 [*Russ. J. Phys. Chem.*, 2002, **77**, No. 5 (Engl. Transl.)].
70. Yu. K. Tovbin, *Zh. Fiz. Khim.*, 2003, **77**, No. 11 [*Russ. J. Phys. Chem.*, 2003, **77**, No. 4 (Engl. Transl.)].

Received September 4, 2002;
in revised form November 26, 2002